applied sciences

MDPI

Article

A Theoretical Method and Model for TBM Tunnelling Trajectory Adjustment

Ruirui Wang * and Lingli Zhang

School of Civil Engineering, Shandong Jianzhu University, Jinan 250101, China; zhanglingli@sujzu.edu.cn
* Correspondence: wangruirui21@sdjzu.edu.cn

Abstract: TBM tunnelling trajectory adjustment is a significant issue in guaranteeing a tunnel project. This paper proposes a theoretical method of trajectory adjustment aimed at synchronously reducing bias angle and distance. The proposed method can be divided into three steps. First, the need for manual intervention in the tunnelling trajectory is determined based on the current bias angle and distance. Next, if manual intervention is required, a theoretical relationship is established using the current bias angle and distance as an input and the rotated angle of the TBM main beam as an output. Finally, a series of constraints according to the normal working conditions of the TBM are incorporated into the method. These constraints ensure that the method remains within the acceptable range of TBM operation. Using mechanical parameters such as the cutterhead diameter and cutter spacing of the TBM used in the sixth section of the Qingdao Metro Project, a model suitable for the project is established, and the model is modified by the tunnelling trajectory data collected in the field. This method provides a reference for TBM drivers to use to correct the tunnelling trajectory while considering the specific conditions of the project.

Keywords: tunnel boring machine; trajectory adjustment; mechanical parameters; theoretical calculation

check for updates

Citation: Wang, R.; Zhang, L. A Theoretical Method and Model for TBM Tunnelling Trajectory Adjustment. *Appl. Sci.* **2023**, *13*, 10876. https://doi.org/10.3390/app131910876

Academic Editors: Lina M. López and Daniel Dias

Received: 30 June 2023
Revised: 13 September 2023
Accepted: 25 September 2023
Published: 30 September 2023

Copyright: © 2023 by the authors. Licensee MDPI, Basel, Switzerland. This article is an open access article distributed under the terms and conditions of the Creative Commons Attribution (CC BY) license (https://creativecommons.org/licenses/by/4.0/).

1. Introduction

The tunnel boring machine (TBM) is a large-scale piece of equipment which is used for excavating tunnels, particularly in hard rock environments. TBMs have gained popularity in tunnel construction and other underground spaces due to their advantages of fast tunnelling, cost-effectiveness, and high levels of security.

However, the working environment of the TBM is underground and covered by surrounding rock, the properties of which are uncertain, making it challenging to accurately determine the TBM's position and control its tunnelling trajectory to align with the planned route [1–3]. Although TBMs are equipped with a measurement system used to measure the tunnelling bias condition compared to the expected trajectory, human experience alone is often insufficient to effectively control the tunnelling trajectory. Consequently, deviations from the intended trajectory can occur, leading to time and economic losses as well as compromised project quality [4].

Hence, controlling the TBM's tunnelling along the expected trajectory is a critical issue in TBM tunnelling and has garnered significant attention from researchers.

Research in the field of TBM trajectory adjustment can be divided into two categories based on the objectives. The first category focuses on controlling the tunnelling direction of the TBM by adjusting the tunnelling parameters, primarily the stroke of thrust and gripper cylinders. For example, Shao et al. built a three-dimensional tunnelling direction-controlling dynamic model which was used to adjust the tunnelling direction according to the need by controlling the thrust and gripper cylinders [5,6]. Zhou et al. used a hybrid method including a convolutional neural network (CNN) and a long-term and short-term memory network (LSTM) to establish a relationship model with multiple tunnelling parameters as the input and the horizontal and vertical tunnelling attitude as the output,

and this model can be used to predict the TBM tunnelling direction [7]. In addition, many researchers, such as Manabe et al., Sugimoto et al., and Festa et al., made efforts with great reference value [3,8–12]. These research studies provide valuable insights and references for TBM trajectory adjustment.

In contrast, the second category focuses on macroscopically designing the tunnelling trajectory in order to make it close to the expected route. For example, Hu et al. established an LSTM real-time tunnelling deviation prediction model. Compared with the model only based on theoretical analysis, the analyzing process of this model includes the geological factors [13]. Zhang et al. incorporated the Grey prediction (PID) strategy into the TBM trajectory adjustment and built a trajectory adjustment dynamic model which can optimize the tunnelling trajectory in real time by analyzing the difference between the current and expected tunnelling direction [14]. Xie et al. proposed a strategy for controlling the TBM tunnelling trajectory using the hydraulic thrust system principle and hydraulic load simulation test, and the tunnelling direction and position were well controlled using this method [15]. Wang et al. conducted kinematic analysis of the thrust system of the TBM and developed a control system for the multiple thrust cylinder system of the TBM, and this is useful for controlling the TBM attitude [16]. In addition, other studies conducted by researchers are helpful with this problem [7,17–24].

This research belongs to the second category, aiming to optimize the tunnelling trajectory to closely match the expected route and simultaneously eliminate deviations in distance and direction. The proposed method can obtain a feasible region of the rotated angle of the main beam used to adjust the tunnelling trajectory according to the current bias angle and distance. The method consists of three steps. First, the need for manual intervention in the tunnelling trajectory is determined based on the mode of tunnelling attitude. Then, in cases requiring manual intervention, a theoretical relationship between the current bias condition (bias angle and distance) and the rotated angle of the main beam used for controlling the tunnelling trajectory is established. Finally, several constraints are established based on the requirements for the normal operation of the TBM, and a feasible region for selecting the rotated angle is obtained. This feasible region serves as a reference for the TBM driver to adjust the tunnelling trajectory, allowing them to select a suitable rotated angle within the obtained feasible region.

This paper is organized as follows: Section 2 introduces the TBM tunnelling trajectory adjustment method. In Section 3, the method is applied to the TBM of the sixth section of the Qingdao Metro Project, and a detailed trajectory adjustment model is formed. Section 4 adjusts the model by comparing the calculated results of the proposed model and the field tunnelling data. Section 5 concludes this paper.

2. Method

2.1. Overview of the Method System

In actual projects, different types of TBMs use different trajectory adjustment methods. Double-shield TBMs typically adjust the main beam direction by changing the stroke of the thrust cylinder systems, which in turn adjusts the tunnelling direction, while open-type TBMs adjust the main beam direction and tunnelling direction by changing the stroke of the left and right gripper cylinders. Regardless of the TBM type, the common goal of trajectory adjustment is to change the direction of the main beam based on the existing tunnelling bias condition, as shown in Figure 1 [21]. This process is conducted based on human subjective experience, making it challenging to control the accuracy and efficiency of trajectory adjustment. This paper proposes a theoretical method to quantify this task. The tunnelling bias condition of the TBM, including the bias angle and bias distance in both the horizontal and vertical directions, is quantitatively described using four physical quantities, as shown in Figure 1. Correspondingly, a suitable rotated angle of the main beam will be obtained by the proposed method, which is directly related to the tunnelling trajectory.

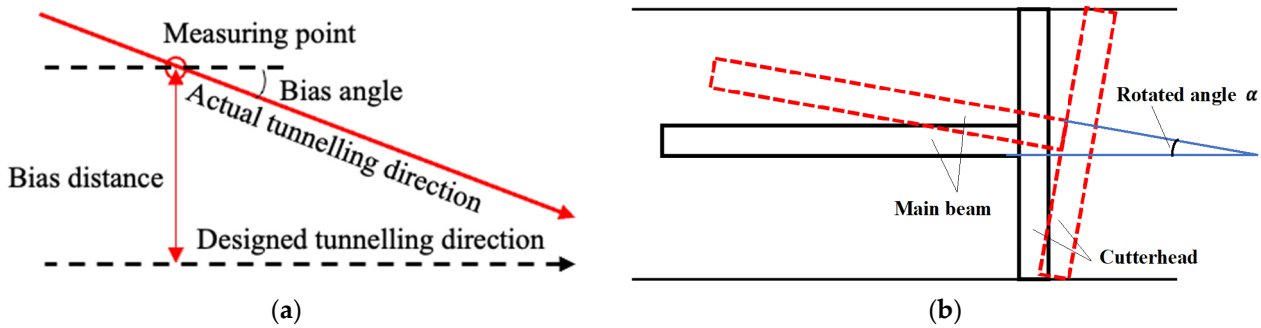


Figure 1. Flowchart of the TBM tunnelling trajectory: (**a**) bias angle and distance; (**b**) rotated angle of the main beam used to control tunnelling trajectory.

Ideal TBM trajectory adjustment should have two key characteristics. First, it should be infrequent. The resultant force and tunnelling direction should not require frequent adjustments. For TBM tunnelling, there is a certain distance permitted between the actual and expected measured point. Tunnelling within the permitted deviation can be achieved without human intervention. Additionally, the direction of the main beam should be considered during trajectory adjustment. If the deviation directions of the key point and main beam are opposite, meaning that the TBM can naturally and gradually return to the expected trajectory, then the tunnelling state can be maintained. For example, if the measured point deviates to the left of the expected position, while the main beam slightly deviates to the right, the measured point will naturally move to the right, reducing its deviation without the need for human control. The second key characteristic is being smooth and progressive. The angle deviation of the TBM main beam and cutterhead should be limited. Excessive angle deviation results in a large bias moment acting on the cutterhead. This can be harmful to the cutters, especially the cutter located on the edge of the cutterhead.

According to the above considerations, a TBM trajectory adjustment method with constraints is proposed. The method consists of three steps:

(1) Judging the current tunnelling state. In this step, the horizontal and vertical deviation of the measured point and main beam are used to judge the necessity of trajectory adjustment. There are two criteria for judgement; one is if the actual deviation from the measured point meets the requirements of the permitted value, and the other is if the deviation direction of the measured point and main beam are opposite. Only when neither of these criteria are met does the tunnelling need human controlling and the method continue. This step is described in Section 2.2.

(2) Building and conducting the TBM trajectory adjustment model. Based on the field-measured data, the theoretical relationship between the TBM controlling parameter (bias angle of the main beam) and the trajectory parameters (bias angle and distance) are researched. This step is described in Section 2.3.

(3) Constructing the constraints of the main beam bias angle. In this step, the bias angle of the main beam and cutterhead is controlled in order to protect the cutters from abnormal wear. Specifically, a permitted difference of the penetration of adjacent cutters is determined. Combining this difference value with the fixed cutter spacing, the permitted bias angle of the main beam and cutterhead can be calculated, which is used as a constraint in the process of calculating the bias angle of the main beam. This step is described in Section 2.4.

2.2. Judge the Current Tunnelling State

In this paper, permitted deviation and the consistency between angles and distances are used as the two indexes to judge whether trajectory adjustment is necessary for the TBM. When the two indexes are not satisfied, trajectory adjustment is conducted by controlling

the thrust ratio of the four groups of thrust cylinders, which are located on the top, bottom, left, and right of the main beam. The two judging indexes are described in detail as follows.

Index 1: Limited by the tunnelling accuracy, it is difficult to completely excavate the tunnel along the designed trajectory. A small deviation is permitted, and the permitted deviation is used to judging whether trajectory adjustment is required. Usually, there are measurement points located on the TBM shield, and the distance between the actual and designed location of the measurement points, recorded as d_h and d_v, are used to characterize the deviation distance of the TBM in this paper.

Index 2: Distance and angle are used to describe the tunnelling deviation and determine the necessity of trajectory adjustment. For example, if the measurement points are located left of the designed position, while the actual tunnelling direction is right compared with the designed route, as shown in Figure 2a, then the bias distance will decrease with the continued excavation of the TBM. On the contrary, if the measurement point is located to the right of the designated position, as shown in Figure 2b, then the bias distance will increase, and the tunnelling trajectory needs manual intervention. Overall, if the bias angle and distance consistently deviate from the desired direction, then the TBM cannot automatically return to the design route with further excavation, and manual intervention is required for trajectory adjustment.

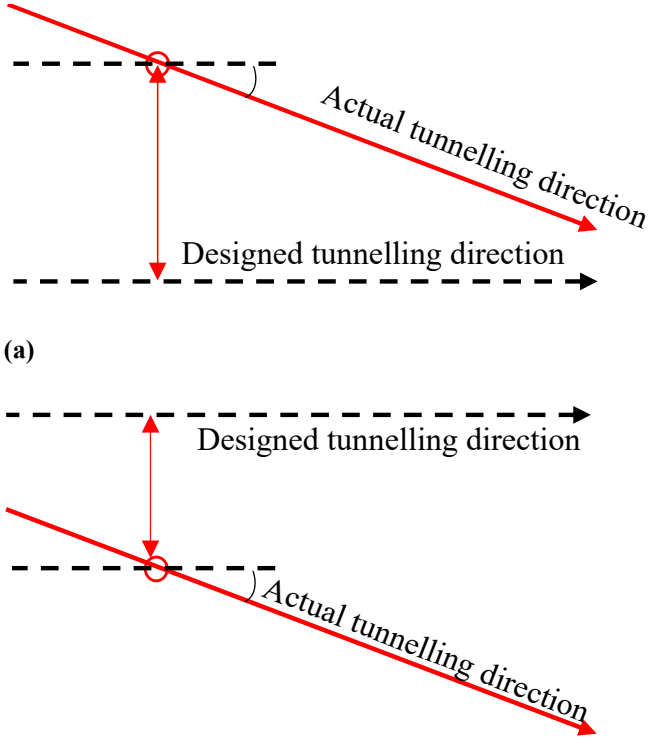


Figure 2. Flowchart of the consistency between the bias angle and distance; (**a**) same direction, (**b**) opposite.

2.3. Excavation Trajectory Design

This step aims to solve this problem and design a scientific and safe route to adjust the TBM so as to excavate along the expect trajectory. With this target, a three-stage trajectory adjustment strategy is proposed and depicted in Figure 3.

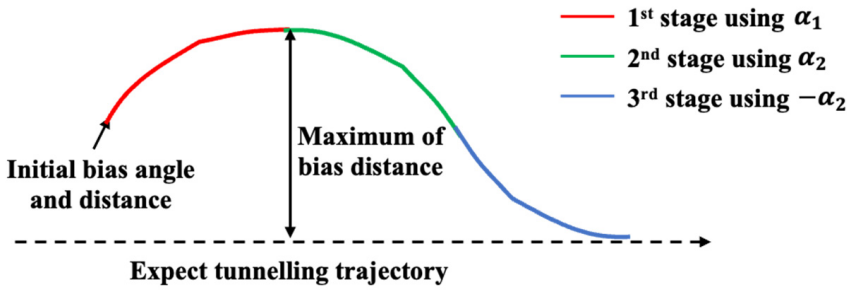


Figure 3. The flow chart of the trajectory adjustment strategy with three stages.

In this method, the known variables, i.e., the basis of the trajectory adjustment, are the initial bias angle θ_1 and distance d_0. The controlled index is the rotated angle of the main beam in the three stages and is recorded as α_1, α_2, and α_3. On this basis, the curvature and the curvature radius of the tunnelling trajectory should be determined.

The TBM tunnelling can be divided into several sections with the same length l which are commonly referred to as "rings" in the actual project. Due to the slightly rotated angle of the main beam, the TBM's turning trajectory can be approximated as a broken line composed of multiple short lines (Figure 4), and the included angle difference of the adjacent line is α. On this basis, the curvature K and curvature radius ρ can be calculated by the following equation.

$$\sin \alpha_i = \frac{l}{2 \cdot \rho_i} \tag{1}$$

$$K_i = \frac{1}{\rho_i} = \frac{2 \cdot \sin \alpha_i}{l} \tag{2}$$

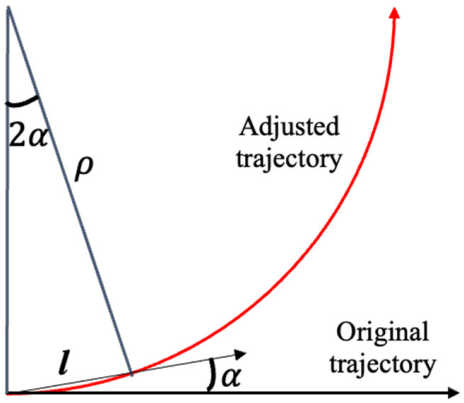


Figure 4. Flowchart of calculating the tunnelling curvature.

The curvature of the first-stage tunnelling trajectory K_1 can be calculated using the rotated angle of the main beam α_1. Further, the length of the first-stage tunnelling trajectory s_1 and the bias distance d_1 can be calculated as

$$s_1 = \frac{\theta_1}{K_1} \tag{3}$$

$$d_1 = d_0 + d_1' = d_0 + \frac{(1 - \cos \theta_1)}{K_1} \tag{4}$$

Similarly, in the second and third stages, a fixed curvature is also used to adjust the bias distance. In detail, the values of the curvature of the second and third stages are the same, but their directions are opposite. Therefore, the second and third stages can be regarded as a pair of inverse processes; in other words, when the measurement point of the

TBM reaches half of the bias distance d_1, the TBM tunnelling curvature turns to the opposite direction, and the third stage starts, while the bias angle is recorded as θ_2. The rotated angle of the main beam and the tunnelling curvature in the second stage are recorded as α_2 and K_2.

The second and third stages are a pair of reciprocal process, so their reductions of the TBM bias distance are the same and are recorded as d'_2 and d'_3. Ideally, when the bias angle of the TBM reaches 0, the bias distance reaches 0 exactly. With this target, the relationship between the increment of bias distance in each stage d'_1, d'_2, and d'_3 and the initial bias distance d_0 can be expressed by the following equations.

$$d'_2 = d'_3 = \rho_2 \cdot (1 - \cos\theta_2) = \frac{(1 - \cos\theta_2)}{K_2} \tag{5}$$

$$0 = d_0 + d'_1 - d'_2 - d'_3 = d_0 + \frac{l \cdot (1 - \cos\theta_1)}{2 \cdot \sin\alpha_1} - \frac{l \cdot (1 - \cos\theta_2)}{\sin\alpha_2} \tag{6}$$

Ideal trajectory adjustment should satisfy Equation (6), where d_0 and θ_1 are the known variables, namely the mentioned bias distance and bias angle. The selection of α_1, α_2, and θ_2 requires manual intervention. This equation is the expression of the optimized tunnelling trajectory. Specifically, the rotated angles of the main beam used in the second and third stages are equal, but their direction is opposite. It is necessary to adjust the rotated angle to zero at the transition between the second and third stages. During this transition, the TBM needs to excavate a short distance while keeping the main beam along the tunnelling direction. Compared to the total distance of the trajectory adjustment, the distance of the transition is relatively small and is ignored in the construction of the proposed model.

2.4. Constraints of the Main Beam Bias Angle

In this section, constraints for the main beam bias angle are introduced when the two criteria discussed in Section 2.2 are not satisfied. Equation (6) represents the expression of the optimized tunnelling trajectory. However, it is evident that this equation has multiple solutions. Therefore, three types of constraints are established in this section to limit the range of solutions and address this issue.

1. Constraints of the initial and maximum bias distance

Generally, manual trajectory adjustment is only required when the bias distance reaches a certain threshold, represented by $d_{0\min}$. Additionally, throughout the entire tunnelling process, the bias distance is limited and cannot exceed $d_{1\max}$. The purpose of $d_{0\min}$ is to limit the frequency of trajectory adjustments, while $d_{1\max}$ ensures the quality of the tunnelling trajectory. In the proposed method, these constraints can be expressed using the following equations. The values of $d_{0\min}$ and $d_{1\max}$ are generally determined by the construction enterprise based on the characteristics of the TBM and tunnel [25,26].

$$\begin{cases} d_0 \geq d_{0\min} \\ d_1 \geq d_{1\max} \end{cases} \tag{7}$$

2. Constraints of the main beam rotated angle

The protection of TBM cutters should be considered during trajectory adjustment. To address this, a constraint is proposed in this paper. The TBM cutterhead is equipped with dozens of cutters arranged at equal intervals in the radius direction. To ensure the even distribution of tunnelling load among different cutters and protect them from abnormal damage, the penetration differences between adjacent cutters are limited, which is also a key reason for frequently updating cutters. During trajectory adjustment, the cutterhead will rotate slightly with the main beam, forming an included angle between the cutterhead and tunnel face, which leads to penetration differences between cutters in different positions. The relationship between the rotated angle of the cutterhead and the

penetration of each cutter is illustrated in Figure 5. The permitted penetration differences between adjacent cutters are recorded as p', and the cutter spacing is recorded as s. The permitted rotated angle of the main beam, θ', which is also the cutterhead, can be calculated using Equation (8).

$$\alpha_i = \tan^{-1} \frac{p'}{s} \tag{8}$$

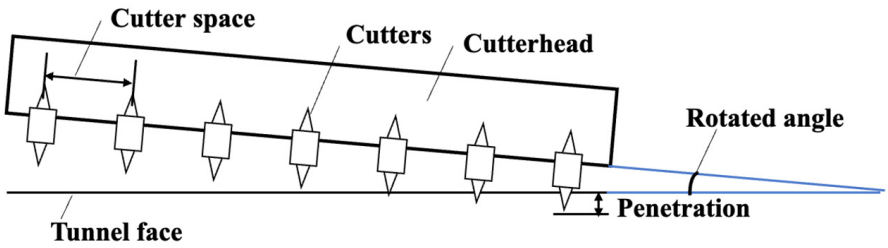


Figure 5. Flowchart of the relationship between the rotated angle of the cutterhead and TBM penetration.

3. Constraint of the total tunnelling distance

The total length of tunnelling deviation from the expected trajectory is always limited, as the TBM needs to return to the expected trajectory as quickly as possible. The route length is measured as a straight line. In this method, the bias angle of the TBM is assumed to be small enough to be ignored, and the tunnelling length deviating from the expected trajectory is considered to be approximately the sum of s_1, s_2, and s_3. The total length of tunnelling deviation from the expected trajectory, $s_{\max}$, can be expressed using the following equation.

$$s_1 + s_2 + s_3 \leq s_{\max} \tag{9}$$

3. Case Study

3.1. Project Overview

To modify and improve this research, the area from Heluobu station to Zhuamashan station in the sixth section of the Qingdao Metro Project is investigated, which is located in Shandong Province, China. This area covers a total length of approximately 1750 m and was excavated by a TBM with a diameter of 6.0 m from the mileage of YDK48+844 to YDK50+593. The tunnel runs from northwest to southeast. The landform along the tunnel mainly consists of hills. The depth of the tunnel is not exceeding 50 m. According to the China hydropower classification (HC) method, the surrounding rock along the tunnel mainly consists of class II and III rock. The tunnel has a large altitude range, ranging from 15 to 30 m, which poses substantial difficulty to the vertical trajectory adjustment of the TBM. Part of the geological profile of the project is shown in Figure 6.

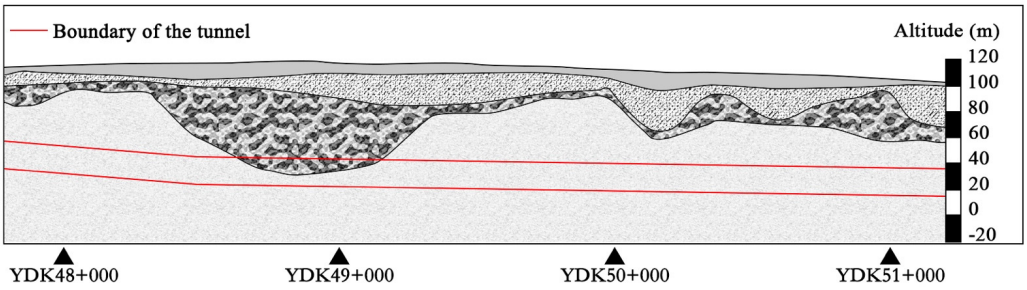


Figure 6. Part of the sixth section of the Qingdao Metro Project geological profile.

3.2. Trajectory Adjustment Model

In order to apply the proposed method for TBM trajectory adjustment, we need to know the values of several constraints introduced in Section 3.2. These constraint values vary depending on the specific TBM used. By combining the design parameters of the TBM

used in the sixth section of the Qingdao Metro Project with the actual project requirements, we obtain the values of these constraints and establish the TBM trajectory adjustment model. These constraints and their values are summarized in Table 1. Among them, the main beam rotated angle is calculated according to the limitation of the penetration difference between adjacent cutters (5 mm) and the actual cutter spacing (73 mm), and the total tunneling distance is set to one ring.

Table 1. The constraint values suitable for the TBM used in the sixth section of the Qingdao Metro Project.

d_{0min}	d_{1max}	α_i	s_{max}
40 mm	60 mm	6.82×10^{-2}	1800 mm

When the values of these constraints and the initial bias angle and distance are known, reasonable tunnelling trajectories can be calculated using the method proposed in Section 2. The main beam rotated angles (α_1 and α_2) are used to express the tunnelling trajectory. As an example, assuming an initial bias angle of 9 mm/m and a bias distance of 40 mm, multiple trajectories meeting the constraints can be obtained through calculation. Some of these trajectories are listed in Table 2.

Table 2. Partly combinations of the calculated trajectory parameters.

$\alpha_1(\times 10^{-2})$	ρ_1 (mm)	s_1 (mm)	d_1 (mm)	$\alpha_2(\times 10^{-2})$	ρ_2 (mm)	θ_2	s_2 (mm)	$s_1+ s_2+ s_3$ (mm)
6.82	13,201.45	118.81	40.53	6.82	13,201.45	5.54×10^{-2}	731.61	1582.03
6.82	13,201.45	118.81	40.53	5.16	17,435.39	4.82×10^{-2}	840.60	1800.00
2.41	37,420.08	336.78	41.52	6.82	13,201.45	5.54×10^{-2}	731.61	1800.00
4.00	22,506.00	202.55	40.91	5.77	15,597.16	5.12×10^{-2}	798.73	1800.00
5.00	18,007.50	162.06	40.72	5.47	16,470.90	4.97×10^{-2}	818.97	1800.00

Table 2 shows five combinations of α_1 and α_2. In the first combination, α_1 and α_2 reach their permitted maximum value of 6.82×10^{-2}, resulting in a rapidly corrected trajectory with a total tunnelling distance of 1582.03 mm. However, the trajectory adjustment process could be slower and steadier. In the second and third combinations, the total tunnelling distance reaches its maximum of 1800 mm. In the second combination, α_1 is fixed at its maximum, while in the third combination, α_2 is fixed at its maximum. The values of α_2 in the second combination and α_1 in the third combination are calculated to be 5.16×10^{-2} and 2.41×10^{-2}, respectively.

Figure 7 illustrates the relationship between α_1 and α_2, representing different trajectory adjustment schemes. Each point on the figure represents a combination of α_1 and α_2 as well as a trajectory adjustment scheme. The five black points with numbers correspond to the five schemes listed in Table 2. The dotted lines and curves represent the constraints proposed in this paper. The orange area is formed by the overlapping of the red and yellow areas, indicating that the schemes in this area do not satisfy both the main beam rotated angle and total tunnelling distance constraints. Only the schemes located in the green area satisfy all of the constraints and are permitted. It is important to note that these results are based on the assumed condition with an initial bias angle of 9 mm/m and a bias distance of 40 mm. The results will differ for different conditions, including the location of each constraint and the area. In other words, the model can calculate the reasonable area of the trajectory adjustment scheme based on the initial bias angle and distance, thereby providing the TBM main driver with a reference.

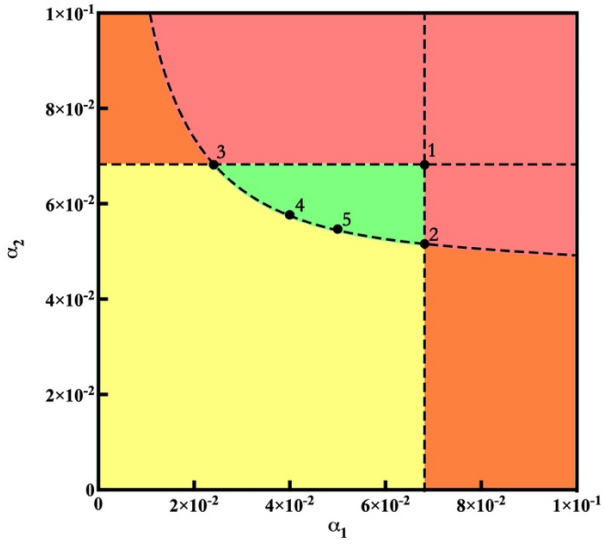


Figure 7. Reasonable trajectory adjustment scheme suitable for the example.

4. Model Modification

In order to modify and validate the proposed method and model, a partial dataset of horizontal and vertical trajectory data from the investigated area is collected and studied. Data collection and analysis were conducted on a ring-by-ring basis. Specifically, the horizontal and vertical bias angles and distances, as well as the main beam rotated angle of each ring, were recorded as a set of data for further analysis. The proposed method's two judgment criteria are applied to the data, extracting only the samples that require manual intervention for further study. The tunnelling trajectories of these samples were then calculated using the proposed model and were compared to the actual trajectories controlled by the TBM main driver.

4.1. Data Preparation

Based on the sixth section of the Qingdao Metro Project, the bias angle and distance in the horizontal and vertical direction were recorded for a total of 57 rings. Positive and negative values represent biases in different directions. In the horizontal direction, positive values indicate bias to the right of the expected trajectory, while negative values indicate bias to the left. In the vertical direction, positive values indicate that the TBM is above the expect trajectory, while negative values indicate that it is below. These data are used to judge whether manual intervention is required for the tunnelling trajectory based on the proposed criteria. The bias angle and distance for the 57 rings are shown in Figures 8 and 9.

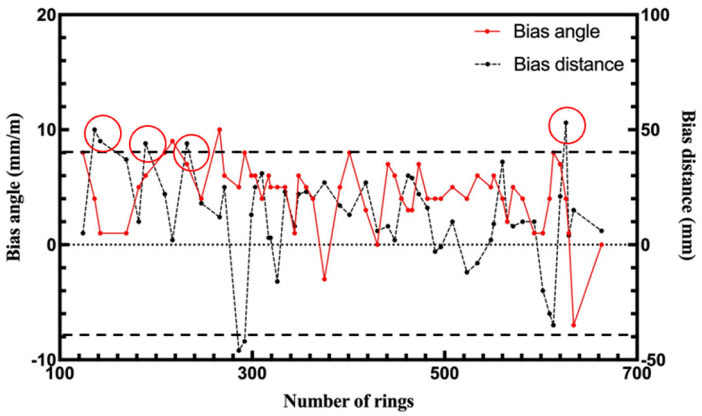


Figure 8. The bias angle and distance in the horizontal direction.

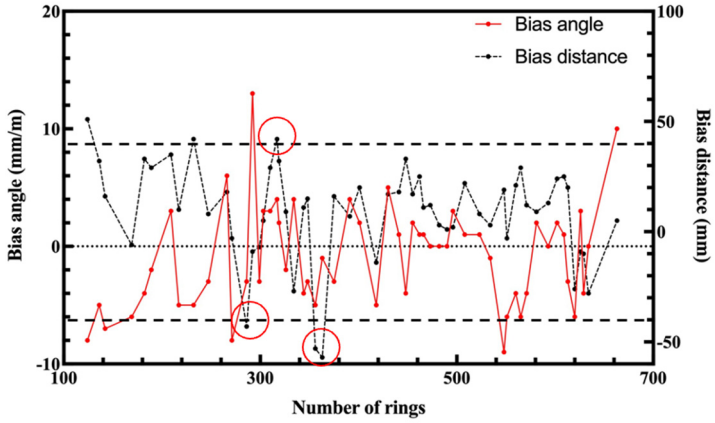


Figure 9. The bias angle and distance in the vertical direction.

Tunnelling trajectories requiring manual intervention must satisfy two criteria. First, their bias distance must exceed 40 mm, and second, their bias angle and distance must be towards the same direction. As observed in Figures 8 and 9, most samples in the horizontal direction have bias distances within the range of −40 mm to 40 mm. Additionally, some remaining samples have opposite bias angles and distances, such as rings 286# and 292#, with bias angles of 5 mm/m and 8 mm/m and bias distances of −46 mm and −42 mm. These samples do not meet the proposed criteria. Therefore, only the horizontal trajectories of rings 136#, 142#, 189#, 232#, and 626# require human intervention and will be further studied using the proposed method and model in Section 4.2. Similarly, the vertical trajectories of samples 286#, 334#, 356#, and 363# are suitable for the method and model, resulting in a total of nine samples listed in Table 3.

Table 3. Basic information about the samples needing human invention using the proposed method.

Number of Rings	Direction	Bias Angle (mm/m)	Bias Distance (mm)
136	Horizontal	4	50
142	Horizontal	1	45
189	Horizontal	6	44
232	Horizontal	7	44
626	Horizontal	4	53
286	Vertical	−3	−43
334	Vertical	4	42
356	Vertical	−5	−53
363	Vertical	−1	−57

4.2. Analysis of the Trajectory Adjustment of the Target Samples

The proposed model is analyzed using nine target samples listed in Table 3, each with a different bias angle and distance. According to their bias angle and distance, corresponding possible combinations of α_1 and α_2 are calculated by the proposed model. Considering that the TBM does not have the function of recording the actual rotated angle of the main beam and the cutterhead α_1 and α_2, in this project, the actual α_1 and α_2 are approximately calculated according to the propulsion stroke of the thrust cylinder. In detail, the TBM is equipped with four groups of thrust cylinders located at the top, bottom, left, and right of the main beam, as Figure 10 shows. In general, the stroke of cylinders in the same group is consistent, while the difference from the stroke of different groups of cylinders results in the included angle between the cutterhead and the tunnel face. Therefore, the rotated angle can be calculated according to the stroke of each group of cylinders and their geometric center, as Equation (10) shows [27].

$$\begin{cases} \alpha_H = \tan^{-1} \frac{s_C - s_A}{d_{AC}} \\ \alpha_V = \tan^{-1} \frac{s_D - s_B}{d_{BD}} \end{cases} \quad (10)$$

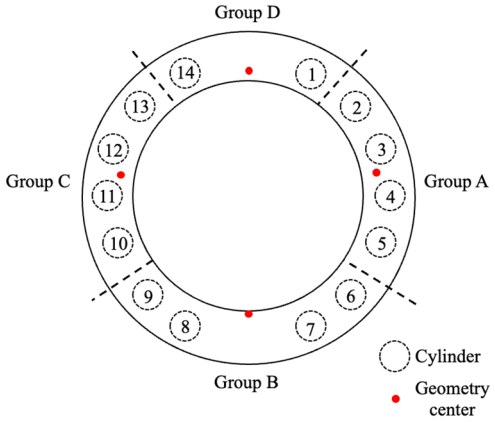


Figure 10. The diagram of the thrust cylinder distribution.

As Equation (10) shows, α_H and α_V represent the rotated angle of the main beam in the horizontal and vertical direction; s_A, s_B, s_C, and s_D represent the cylinder stroke of each group; d_{AC} means the distance between the geometric centers of group A and C; and d_{BD} means the distance between the geometric centers of group B and D. Usually, constant rotated angles of the main beam are used during the excavation process in a single ring. Therefore, α_1 and α_2 are recorded as the same value, i.e., the calculated results of Equation (10). The comparison results of the actual rotated angle of the nine target samples and the corresponding trajectory adjustment feasible region calculated by the proposed model are shown in Figure 11.

As Figure 11a–i shows, the main beam rotated angles used in the actual project of the nine samples are located below their feasible region. According to the analysis from Section 3 of this paper, these samples are located in the yellow area, which means that the tunnelling distances used to correct their tunnelling trajectory are longer than 1800 mm (one ring). In order to verify this conclusion, the changing rules between the bias distance and the tunnelling distance of these target samples are calculated by the proposed method. The results are shown in Figures 12 and 13. Specifically, the bias distances shown in Figures 12 and 13 only represent their absolute value, while their direction information can be found in Table 3.

As Figures 12 and 13 show, all of the tunnelling distances used to correct the bias distance of the target samples are greater than 1800 mm, and this conclusion is consistent with the comparison results of the actual main beam rotated angles and their feasible regions, which are shown in Figure 7. In addition, the tunnelling distances of rings 142# and 232# in the horizontal direction and rings 286# and 334# in the vertical direction are relatively small—less than 2000 mm. Meanwhile, their actual main beam rotated angles are also relatively close to the corresponding feasible regions, which are shown in Figure 11b,d,f,g, respectively. Contrarily, the calculated tunnelling distances of rings 136#, 189#, and 626# in the horizontal direction and rings 356# and 363# in the vertical direction are more than 2000 mm, which is also reflected in Figure 11a,c,e,h,i. In fact, in the actual tunnelling, it is difficult to correct TBM bias within a distance of one ring; longer tunnelling distances are always used. In order to adapt to this situation, in actual tunnelling, more flexible models and feasible regions are needed, and the model should be further enriched and modified.

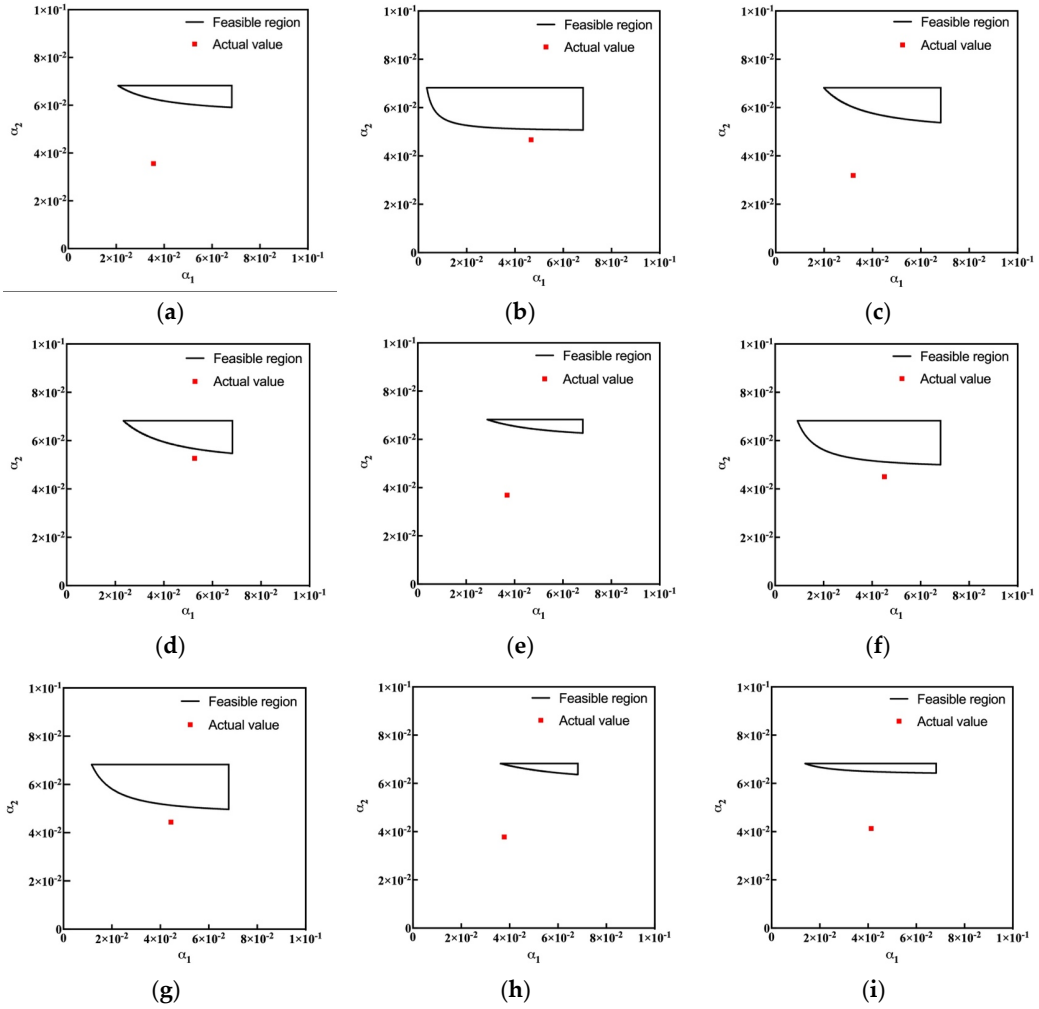


Figure 11. The trajectory adjustment feasible regions and corresponding actual value of the nine target rings. (**a**) The horizontal direction of 136th ring; (**b**) The horizontal direction of 142nd ring; (**c**) The horizontal direction of 189th ring; (**d**) The horizontal direction of 232nd ring; (**e**) The horizontal direction of 626th ring; (**f**) The vertical direction of 286th ring; (**g**) The vertical direction of 334th ring; (**h**) The vertical direction of 356th ring; (**i**) The vertical direction of 363rd ring.

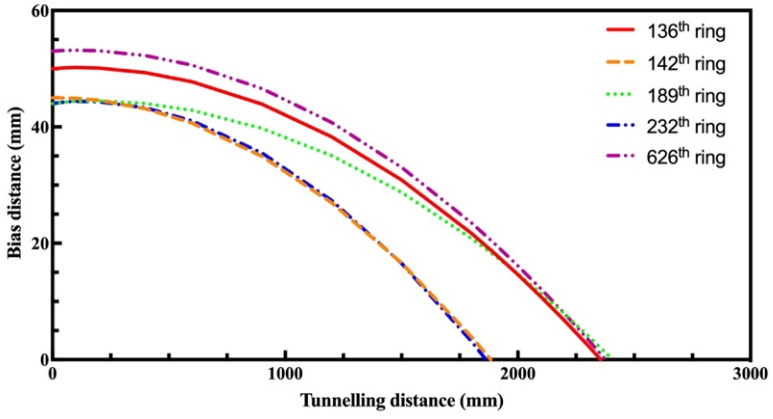


Figure 12. The changing rules between the bias distance in the horizontal direction and the tunnelling distance of the target rings.

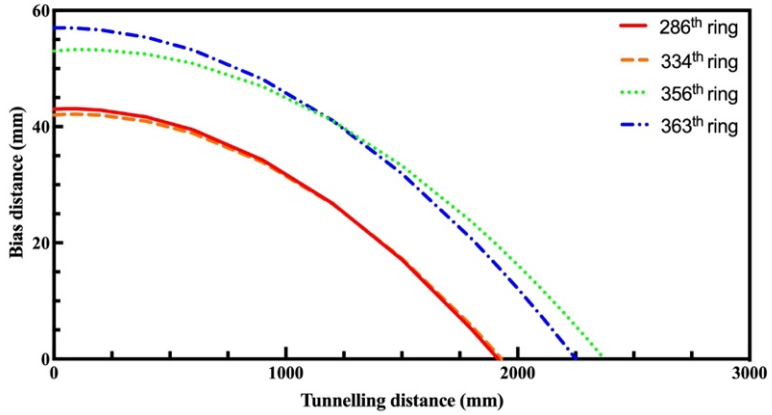


Figure 13. The changing rules between the bias distance in the vertical direction and the tunnelling distance of the target rings.

4.3. Modification of the Proposed Model

According to the field samples, it is found that the feasible region obtained by the proposed model is too small, and the model needs to be modified. The reason for the results is that the constraint of the total tunnelling distance is set to be too strict. To resolve this, the value of this constraint is adjusted to be multiple values, and correspondingly, multiple feasible regions with different levels are obtained. The multiple values of the constraint of total tunnelling distance are set in the range from 1 ring (1800 mm) to 1.5 rings (2700 mm) with the step of 300 mm. Taking the case given in Section 3 as an example, the modified model is changed to the one shown in Figure 14.

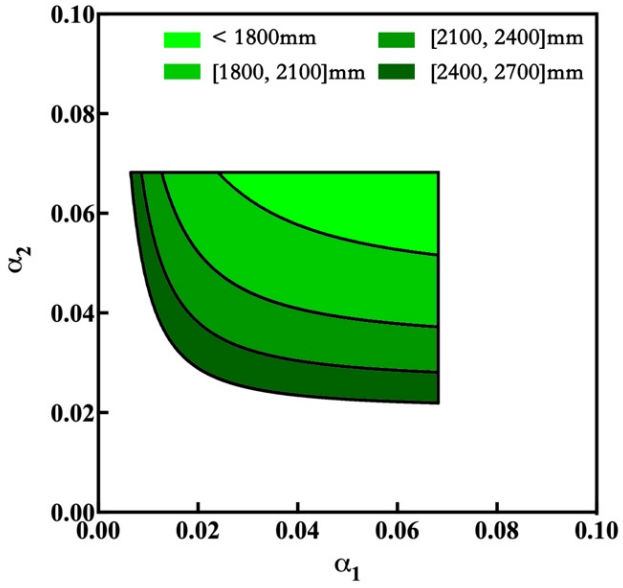


Figure 14. Feasible region calculated by the modified model for the example.

As Figure 14 shows, the feasible region calculated by the modified model is divided into three parts with different filled colors, and these parts represent potential combinations of α_1 and α_2 within the different total tunnelling distances. Among them, the lightest green region represents trajectory adjustment schemes in which the total tunnelling distance used for trajectory adjustment is less than 1800 mm—this is the same as the feasible region calculated by the originally proposed model—while the remaining three regions filled in different depths of green represent total tunnelling distance ranges of [1800, 2100] mm, [2100, 2400] mm, and [2400, 2700] mm, respectively. Compared with the originally proposed

model, a looser constraint is used in the modified model, which results in more ranges for trajectory adjustment and makes the results closer to the field data.

5. Discussion

5.1. Existence of the Solution Space of α_1 and α_1

In the proposed model, three constraints are developed to limit the selection range of α_1 and α_2. In general, there is a solution space of α_1 and α_2 that satisfies the three constraints at the same time. However, when the bias distance and angle reach a high level, the three constraints cannot be satisfied at the same time, and the proposed method is not suitable for this situation. In this section, the above cases and the applicability of the model will be researched.

According to the three stages of the proposed trajectory adjustment method, the bias distance reaches its maximum at the end of the first stage, and the maximum is not permitted to exceed 60 mm. Based on Equation (6), the maximum bias distance is related to the original bias distance, original bias angle, and the rotated angle of the first stage α_1. In this section, the maximum is set to 60 mm, the α_1 is set to its maximum—which is calculated by Equation (6)—and a relationship between the original bias angle and bias distance can be calculated. This relationship represents a series of situations, and in these situations, the permitted maximum of α_1 is used to adjust the TBM, and the maximum bias distance reaches 60 mm. Further, if the original bias distance and angle are larger than these situations, then the maximum bias distance will exceed 60 mm or the α_1 will be larger than the permitted value; in other words, the proposed constraints cannot be satisfied at the same time, and the proposed model is not suitable for these situations. The above relationship between the initial bias angle and distance is shown in Figure 15.

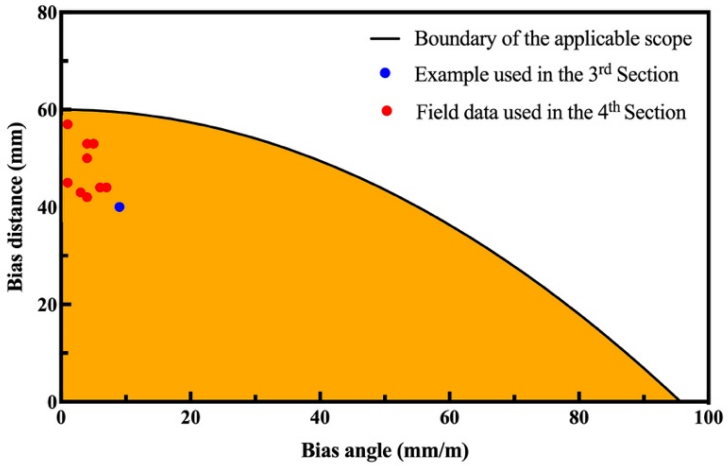


Figure 15. Combination of the bias angle and distance suitable for the proposed model.

As Figure 15 shows, the curve indicates a series of critical situations. If the original bias angle and distance are located on this curve, and the rotated angle α_1 is set to its maximum, then the maximum of the bias distance exactly reaches 60 mm. In addition, in the situations below to the curve, more flexible α_1 can be used to adjust the trajectory of TBM, and the proposed method and model is suitable for these situations. On the contrary, the proposed method and model is not suitable for the situations above the curve.

5.2. Limitation and Further Researches

This research proposed a theoretical method of TBM trajectory adjustment, and it is modified by the field data to be suitable for actual projects. However, this research still has some limitations which require further research to be corrected. The main limitations are summarized as follows.

1. In the proposed method, rational rotated angles of the main beam are used to deal with different initial TBM bias conditions. However, the rotated angle cannot be directly controlled by the TBM drivers and is instead indirectly controlled by controlling the stroke of the main thrust cylinder system. Therefore, the results of this research are only a reference for TBM tunnelling and cannot be directly used in the field. To address this limitation, the relationship between the thrust cylinder strokes and the rotated angle of main beam should be studied, and this will be an important part of our further studies.
2. Considering the complexity of TBM trajectory adjustment, the tunnelling route in this paper is assumed to be straight line, which is the most common situation in actual projects. However, there are still some conditions in which the TBM is tunnelling along curves. For curve trajectories, the proposed method is not suitable, and a more perfect theoretical method suitable for curve trajectories should be further researched.

6. Conclusions

This study introduces a theoretical method for adjusting the tunnelling trajectory of a TBM. It calculates a feasible region for the rotated angle of the main beam, which controls the tunnelling trajectory based on the current bias angle and distance. The model is developed using the mechanical parameters of the TBM used in the sixth section of the Qingdao Metro Project and is validated and refined using field trajectory data from the same project. The main conclusions of this study are as follows.

A method for adjusting the TBM tunnelling trajectory is proposed, and it takes the current bias angle and distance as an input and determines the rotated angle of the main beam as an output. Through theoretical calculations, the relationship between the input and output is established. Additionally, a set of constraints is proposed based on the normal working conditions of the TBM, limiting the feasible solutions to a specific region known as the feasible region. The calculated feasible region can serve as a reference for TBM drivers to control the tunnelling trajectory, thereby eliminating deviations in distance and direction.

The proposed method involves several unknown variables that represent the TBM's mechanical parameters, such as the cutterhead diameter and cutter spacing. These unknown variables are determined based on the TBM used in the sixth section of the Qingdao Metro Project, and a trajectory adjustment model is developed accordingly. To test this model, an example with an assumed bias angle and distance is presented, and the corresponding feasible region is calculated.

Furthermore, trajectory data are collected from the same project in order to test and refine the proposed model. The results indicate that the constraints on the total tunnelling distance used in the original model are too strict, resulting in the rotated angle of the main beam in the field falling outside the feasible region. Therefore, a modified model with looser constraints is proposed, incorporating multiple levels of feasible regions based on the difference in total tunnelling distance.

These findings contribute to the understanding and practical application of TBM tunnelling trajectory adjustment, providing valuable insights for future projects.

Author Contributions: Methodology, R.W.; validation, R.W. and L.Z.; formal analysis, R.W. and L.Z.; field investigation, R.W. and L.Z.; data collection, R.W. and L.Z.; writing—original draft preparation, R.W. and L.Z.; writing—review and editing, R.W. and L.Z.; writing—figures and tables, L.Z.; funding acquisition, R.W.. All authors have read and agreed to the published version of the manuscript.

Funding: The research was funded by the Natural Science Foundation of Shandong Province (No. ZR202103010903) and the doctoral fund of Shandong Jianzhu University (No. X21101Z).

Institutional Review Board Statement: Not applicable.

Informed Consent Statement: Not applicable.

Data Availability Statement: The data presented in this study are available on request from the corresponding author. The data are not publicly available due to the requirements of the third party, also the partner of this paper.

Conflicts of Interest: The authors declare no conflict of interest.

References

1. Festa, D.; Broere, W.; Bosch, J. Kinematic behaviour of a tunnel boring machine in soft soil: Theory and observations. *Tunn. Undergr. Space Technol.* **2015**, *49*, 208–217. [CrossRef]
2. Lyu, H.; Shen, S.; Zhou, A.; Yang, J. Perspectives for flood risk assessment and management for mega-city metro system. *Tunn. Undergr. Space Technol.* **2019**, *84*, 31–44. [CrossRef]
3. Ren, D.; Shen, S.; Arulrajah, A.; Wu, H. Evaluation of ground loss ratio with moving trajectories induced in double-O-tube (DOT) tunnelling. *Can. Geotech. J.* **2018**, *55*, 894–902. [CrossRef]
4. Wu, L.; Qu, F. Discrete element simulation of mechanical characteristic of conditioned sands in earth pressure balance shield tunneling. *J. Cent. South Univ. Technol.* **2009**, *16*, 1028–1033. [CrossRef]
5. Shao, C. Geological Adaptability Control and Rectification Control of Large-Scale Tunneling Equipment. Ph.D. Thesis, Zhejiang University, Hangzhou, China, 2017.
6. Shao, C.; Liao, J.; Liu, Z.; Su, H. Indirect adaptive robust trajectory tracking control of hard rock TBM with load variation of tunneling face. *Chin. J. Mech. Eng.* **2019**, *32*, 34. [CrossRef]
7. Zhou, C.; Xu, H.; Ding, L.; Wei, L.; Zhou, Y. Dynamic prediction for attitude and position in shield tunneling: A deep learning method. *Autom. Constr.* **2019**, *105*, 102840. [CrossRef]
8. Manabe, T.; Tanno, M.; Matsumoto, M.; Yabuta, T. Automatic direction control technique for microtunneling machine. In Proceedings of the IECON Proceedings Industrial Electronics Conference, San Jose, CA, USA, 29 November–3 December 1999; Volume 3, pp. 1295–1300.
9. Sramoon, A.; Sugimoto, M.; Kayukawa, K. Theoretical Model of Shield Behavior During Excavation. II: Application. *J. Geotech. Geoenviron. Eng.* **2002**, *128*, 138–155. [CrossRef]
10. Peng, Z.; Gong, G.; Yang, H.; Liu, T.; Zhang, Z.; Ouyang, X. The Vertical Adjustment System with Angle Closed Loop Control for TBM. In Proceedings of the 12th IEEE/ASME International Conference on Mechatronic and Embedded Systems and Applications (MESA), Auckland, New Zealand, 26–31 August 2016.
11. Yin, X.; Liu, Q.; Huang, X.; Pan, Y. Perception model of surrounding rock geological conditions based on TBM operational big data and combined unsupervised-supervised learning. *Tunn. Undergr. Space Technol.* **2022**, *120*, 104285. [CrossRef]
12. Guo, D.; Li, J.; Jiang, S.; Li, X.; Chen, Z. Intelligent assistant driving method for tunnel boring machine based on big data. *Acta Geotech.* **2022**, *17*, 1019–1030. [CrossRef]
13. Hu, M.; Wu, B.; Bai, X. A real-time shield attitude deviation prediction method based on data drive. In Proceedings of the IEEE 4th Advanced Information Technology, Electronic and Automation Control Conference (IAEAC), Chengdu, China, 20–22 December 2019.
14. Zhang, H. Modeling and Synchronous Control of TBM Gripping-Thrusting-Regripping System. Ph.D. Thesis, Tianjin University, Tianjin, China, 2016.
15. Xie, H.; Duan, X.; Yang, H.; Liu, Z. Automatic trajectory tracking control of shield tunneling machine under complex stratum working condition. *Tunn. Undergr. Space Technol.* **2012**, *32*, 87–97. [CrossRef]
16. Wang, L.; Yang, X.; Gong, G.; Du, J. Pose and trajectory control of shield tunneling machine in complicated stratum. *Autom. Constr.* **2018**, *93*, 192–199. [CrossRef]
17. Shen, X.; Yuan, D. Influence of shield pitch angle variation on shield-soil interaction. *Rock Soil Mech.* **2020**, *41*, 1366–1376. [CrossRef]
18. Wang, P.; Kong, X.; Guo, Z.; Hu, L. Prediction of axis attitude deviation and deviation correction method based on data driven during shield tunneling. *IEEE Access* **2019**, *99*, 163487–163501. [CrossRef]
19. Li, X.; Di, H.; Zhou, S.; Huo, P.; Huang, Q. Effective method for adjusting the uplifting of shield machine tunneling in upper-soft lower-hard strata. *Tunn. Undergr. Space Technol.* **2021**, *115*, 104040. [CrossRef]
20. Ming, Y.; Wei, S.; Ping, H. Dynamic coordinated control of attitude correction for the shield tunneling based on load observer. *Autom. Constr.* **2012**, *24*, 24–29. [CrossRef]
21. Zhang, Z.; Ma, L. Attitude correction system and cooperative control of tunnel boring machine. *Int. J. Pattern Recognit. Artif. Intell.* **2018**, *32*, 1859018.1. [CrossRef]
22. Wada, K.; Sugiyama, H.; Nozawa, K.; Honda, M.; Yamamoto, S. Guidance system for directional control in shield tunneling using machine learning techniques. In Proceedings of the 18th International Conference on Computing in Civil and Building Engineering, ICCCBE, Sao Paulo, Brazil, 18–20 August 2020; pp. 73–88.
23. Xiao, H.; Xing, B.; Wang, Y.; Yu, P.; Liu, L.; Cao, R. Prediction of shield machine attitude based on various artificial intelligence technologies. *Appl. Sci.* **2021**, *11*, 10264. [CrossRef]
24. He, B.; Zhu, G.; Han, L.; Zhang, D. Adaptive-neuro-fuzzy-based information fusion for the attitude prediction of TBMs. *Sensors* **2020**, *21*, 61. [CrossRef] [PubMed]

25. Liu, T.; Gong, G.; Yang, H.; Chen, Y.; Zhu, Y. Trajectory control of tunnel boring machine based on adaptive rectification trajectory planning and multi-cylinders coordinated control. *Int. J. Precis. Eng. Manuf.* **2019**, *20*, 1721–1733. [CrossRef]
26. Li, J.; Jing, L.; Zheng, X.; Yang, C. Application and outlook of information and intelligence technology for safe and efficient TBM construction. *Tunn. Undergr. Space Technol.* **2019**, *93*, 103097. [CrossRef]
27. Wang, K. Research on Performance of TBM Gripping-Thrusting-Regripping Mechanism. Master's Thesis, Tianjin University, Tianjin, China, 2017.

Disclaimer/Publisher's Note: The statements, opinions and data contained in all publications are solely those of the individual author(s) and contributor(s) and not of MDPI and/or the editor(s). MDPI and/or the editor(s) disclaim responsibility for any injury to people or property resulting from any ideas, methods, instructions or products referred to in the content.